Published in final edited form as:
Bioorg Med Chem. 2009 May 15; 17(10): 3536–3542. doi:10.1016/j.bmc.2009.04.011.

Mechanism-Based Inhibitors of Serine Proteases with High Selectivity Through Optimization of S' Subsite Binding

Yi Li[#], **Dengfeng Dou**[#], **Guijia He**[#], **Gerald H. Lushington**[@], and **William C. Groutas**[#,*]
[#]Department of Chemistry, Wichita State University, Wichita, Kansas 67260
[@]Molecular Graphics and Modeling Laboratory, The University of Kansas, Lawrence, KS 66045

Abstract

A series of mechanism-based inhibitors designed to interact with the S' subsites of serine proteases was synthesized and their inhibitory activity toward the closely-related serine proteases human neutrophil elastase (HNE) and proteinase 3 (PR 3) was investigated. The compounds were found to be time-dependent inhibitors of HNE and were devoid of any inhibitory activity toward PR 3. The results suggest that highly selective inhibitors of serine proteases whose primary substrate specificity and active sites are similar can be identified by exploiting differences in their S' subsites. The best inhibitor (compound *16*) had a k_{inact}/K_I value of 4580 M^{-1} s^{-1}.

Introduction

Chronic obstructive pulmonary disease (COPD) is a multi-factorial inflammatory disorder characterized by alveolar wall destruction, enlargement of the air spaces, and airflow obstruction due to chronic bronchitis and emphysema.[1–3] COPD is the fourth most common cause of death in the U.S., affecting ~16 million people. Current treatment of COPD is symptomatic[4] and there are *no* drugs capable of halting the relentless progression of the disorder, consequently, there is a pressing need for new therapeutic interventions.[5–6]

Many fundamental aspects of COPD pathogenesis are poorly understood, including the molecular mechanisms which underlie the initiation and progression of the disorder. It is generally recognized, however, that the disorder involves the interplay of multiple events and mediators, including oxidative stress,[7–8] alveolar septal cell apoptosis,[9–10] a protease/antiprotease imbalance,[11–12] and chronic inflammation.[13–14] The relationship between these pathogenic mechanisms is poorly understood. Furthermore, an array of serine (neutrophil elastase, proteinase 3), cysteine (cathepsin S) and metallo- (MMP-1, MMP-9, MMP-12) proteases released by neutrophils, macrophages and T lymphocytes contribute to the degradation of lung connective tissue and mediate a multitude of signaling pathways associated with the pathophysiology of the disorder. The precise function(s) of these proteases is unknown, consequently, there is a need for a better definition of which proteases and protease actions, as well as which other enzymes, are of importance in COPD pathogenesis.[15]

*author to whom correspondence should be addressed, Department of Chemistry, Wichita State University, Wichita, KS 67260, Tel. (316) 978 7374; Fax: (316) 978-3431, e-mail: bill.groutas@wichita.edu.

Agents that can be used to delineate the precise role(s) of proteases implicated in COPD by modulating selectively their activity are valuable as mechanistic probes and as potential pharmacological agents. We report herein the results of exploratory studies aimed at probing the S' subsites of the closely-related serine proteases human neutrophil elastase (HNE) and proteinase 3 (PR 3) via the utilization of inhibitor (I) (Figure 1).

Chemistry

Compounds ***8–16*** were synthesized using the general reaction sequence shown in Scheme 1. The synthetic routine is fairly tractable and allows facile manipulation of the primary substrate specificity residue R_1 by starting with an appropriate natural (or unnatural) amino acid. Furthermore, the length of the ester chain and the nature of R_3 can be readily varied by using an appropriately-substituted thioether.

Biochemical studies

Progress curve method.[16]

The inhibitory activity of compound **16** was determined using the progress curve method. The apparent second-order inactivation rate constant (k_{inact}/K_I M^{-1} s^{-1}) was determined in duplicate and is listed in Table 1. Typical progress curves for the hydrolysis of MeOSuc-AAPV-pNA by HNE in the presence of inhibitor **16** are shown in Figure 2. Control curves in the absence of inhibitor were linear. The release of p-nitroaniline was continuously monitored at 410 nm. The pseudo first-order rate constants (k_{obs}) for the inhibition of HNE by **16** as a function of time were determined according to eq (1), where A is the absorbance at 410 nm, v_o is the reaction velocity at t = 0, v_s is the final steady-state velocity, k_{obs} is the observed first-order rate constant, and A_o is the absorbance at t = 0. The k_{obs} values were obtained by fitting the A versus t data to eq 1 using nonlinear regression analysis (SigmaPlot, Jandel Scientific). The second order rate constants (k_{inact}/K_I M^{-1} s^{-1}) were then determined by calculating $k_{obs}/[I]$ and then correcting for the substrate concentration using eq 2. The apparent second-order rate constants (k_{inact}/K_I M^{-1} s^{-1}) were determined in duplicate and are listed in Table 1.

$$A=v_s t+\left\{(v_o - v_s)(1 - e^{-k_{obs}\, t})/k_{obs}\right\}+A_o \quad (1)$$

$$k_{obs}/[I]=(k_{inact}/K_I)[1+[S]/K_m] \quad (2)$$

Incubation method

The inhibitory activity of compounds ***8–15*** was determined by the incubation method and is expressed in terms of the bimolecular rate constant $k_{obs}/[I]$ M^{-1} s^{-1}. Briefly, HNE was incubated with excess inhibitor and the loss of enzymatic activity was followed by withdrawing aliquots at different time intervals and assaying for enzymatic activity. The observed rate constant (k_{obs}) was then calculated according eq 3 below, where [I] is the concentration of the inhibitor in the incubation mixture and $[E]_t/[E]_o$ is the amount of active enzyme remaining at time t.

$$\ln([E]_t/[E]_o) = - k_{obs} t \quad (3)$$

Using inhibitor **9** as a representative member of this series, saturation kinetics was demonstrated by determining k_{obs} over a range of inhibitor concentrations and re-plotting the data as $1/k_{obs}$ versus 1/[I] according to eq 4 below. Saturation

$$1/k_{obs} = (K_I/k_{inact})(1/[I]) + 1/k_{inact} \quad (4)$$

is indicated by the intersection of the experimental line at the positive y-axis (Figure 3) and under these conditions ($[I] << K_I$), $k_{obs}/[I] \approx k_{inact}/K_I$.[17]

Results and Discussion

Inhibitor Design Rationale

The design of inhibitor (I) was based on the following considerations: (a) the 1, 2, 5-thiadiazolidin-3-one 1, 1 dioxide scaffold is a powerful and versatile core structure that is well-suited to the design of mechanism-based inhibitors of serine proteases;[18] (b) the heterocyclic scaffold makes possible the optimization of potency and selectivity by docking to the active site of a target protease in a substrate-like fashion, exploiting multiple binding interactions with both the S and S' subsites; (c) inhibitors based on this scaffold can be used to probe and exploit binding interactions with the S' subsites. This is particularly important with respect to the design of inhibitors of serine proteases that have a very similar primary substrate specificity (S_1),19 such as, for example, HNE and PR 3, and differ primarily in the makeup of their S' subsites; (d) the neutrophil-derived serine proteases elastase and proteinase 3 have been implicated in COPD.20 Indeed, administration of HNE or PR 3 produces emphysema in animals,21 however, the precise role they play in COPD has not been clearly defined; (e) HNE is a basic, 218 amino acid single polypeptide glycoprotein (M_r 29,500) that is highly homologous (54%) to PR 3. The two enzymes have an extended binding site and prefer hydrophobic substrates/inhibitors.[22] The S_1-S_4 subsites of PR 3 and HNE are very similar, with the S_1 subsite of HNE being somewhat bigger than that of PR 3.[23–24] The strong preference of PR 3 for small aliphatic P_1 residues (ethyl, n-propyl) is due to the substitution of Val 190 and Ala 213 in HNE to Ile 190 and Asp 213 in PR 3, respectively, which reduce the size of the S_1 pocket.[25] More importantly, inspection of the X-ray crystal structures of HNE and PR 3 reveals subtle differences in their S' subsites. For instance, Ala 213 and Leu 99 in HNE are replaced by Asp 213 and Lys 99 respectively, in PR 3. Furthermore, the substitution of Leu 143 in HNE to Arg 143 in PR 3, and the presence of Asp 61 make the S' subsites of PR 3 more polar and distinctly different from the hydrophobic HNE subsites. Based on these considerations, it was envisaged that an inhibitor capable of orienting recognition elements toward the S' subsites and having built-in structural flexibility for the introduction of acidic, basic, and/or hydrophobic groups could potentially display greater selectivity toward PR 3 than HNE (or vice versa). Thus, our overarching goal was to obtain highly selective inhibitors of PR 3 and HNE by exploiting differences in the S' subsites of the two enzymes.

Inhibitor (I) was anticipated to inactivate the target protease by docking to the active site and undergoing enzyme-induced ring opening, leading to the formation of a highly reactive sulfonyl imine which, upon further reaction with an active site nucleophilic residue (such as His 57) would ultimately lead to irreversible inactivation of the enzyme (Figure 4).[26] It should be noted that the tetrahedral intermediate depicted in Figure 3 collapses via a 3-aza Grob fragmentation process[27] to yield species (X). Such facile heterolytic fragmentations are common in chemical systems having a nucleophilic atom with a negative charge or unshared electron pair and a leaving group in a 1, 4-relationship (as is the case with the aforementioned tetrahedral intermediate). Furthermore, examples of amide bond cleavage that occurs via a 3-aza Grob fragmentation process are well-precedented (Figure 5).[28]

Incubation of compound ***16*** with HNE led to rapid and time-dependent irreversible inactivation of the enzyme (Figure 6). The inactivated enzyme regained its activity very slowly, indicating the formation of a fairly stable enzyme-inhibitor adduct. The potency of the synthesized

inhibitors was determined either by generating a series of progress curves (Figure 2) and determining the k_{inact}/K_I values by analyzing the data (progress curve method) or by using the incubation method, as described in the Experimental section. Our initial objective was to identify selective inhibitors of PR 3 using derivatives of (I). Thus, based on the known preference of PR 3 for a P_1 residue consisting of a 2–3 carbon chain, most inhibitors synthesized have an n-propyl chain. The selection of an N-methyl group as the P_2 residue was primarily dictated by the results of previous studies which have shown that a methyl group leads to the formation of highly stable enzyme-inhibitor complexes.[18] Activity was optimal when n = 2, consequently all derivatives made had an ester chain of fixed length (unpublished results). The nature of the R_3 group was then varied and the resulting compounds were screened against PR 3 and HNE. Surprisingly, all compounds were devoid of any inhibitory activity toward PR 3 following a 30-minute incubation of inhibitor and enzyme at an [I]/[E] ratio = 500, however, they all showed modest inhibitory activity toward HNE. The lack of inhibitory activity toward PR 3 is not intuitively obvious and may be due to unproductive binding arising from the way the substituted thioether and ester moieties are projecting into the S' subsites. We have previously observed that inhibitory potency is dependent on the pK_a of the conjugate acid of the leaving group (ArS^-), as well as its inherent structure, and that the latter can be modulated to enhance binding affinity through favorable interactions with the S' subsites.[29] With the exception of compound ***16***, the rest of the compounds showed little variation in their inhibitory prowess toward the enzyme. This is probably due to the pK_a of the leaving group since previous studies have shown that leaving groups derived from strong acids ($ArCOO^-$, $ArSO_2^-$) enhance inhibitory activity by several orders of magnitude (18d).

In order to gain further insight and understanding into the observed selectivity shown by this series of inhibitors, molecular docking simulations were performed using inhibitor ***8***. Despite the fact that the active sites of HNE and PR3 are similar, subtle differences in the makeup of the active sites of the two enzymes (vide supra) may result in significantly different binding modes (Figure 7). For binding to HNE, for example, the top-scoring docked conformers of each of the RR, SR and SS stereoisomers were found to orient themselves in a very similar manner (see Figure 8a for comparison of RR and SS stereoisomers) and engaged in multiple attractive interactions, including H-bonding of the ester carbonyl to backbone amide protons from Gly218 and Gly219, and hydrogen bonding of heterocyclic carbonyl (RR) or sulfonyl (SR, SS) to V216 backbone. Of the three stereoisomers examined, the SS enantiomer is predicted to have the greatest affinity for the HNE receptor by a small margin relative to the approximately equivalent RR and SR structures.

For compound ***8*** binding to PR3, stereochemistry may be substantially more important. Docking studies predict that the RR stereoisomer should orient the p-chlorophenyl group into a catalytic site hydrophobic pocket in a manner analogous to the conformation for compound ***8*** bound to HNE, although this leaves a poorer interaction profile with the rest of the active site. However, the SR and SS stereoisomers were not predicted to bind to the PR3 active site in this manner at all. The SS structure, for example, (see Figure 8b) has no group occupying either of the two hydrophobic pockets. Rather, the p-chlorophenyl ring pi-stacks with F192, and the spatial positions of the ester and n-propyl chains are exchanged relative to the analogous RR bound stereoisomer. The SS steroisomer is predicted to yield less favorable affinity with the enzyme than that computed for the RR stereoisomer. Thus, the docking studies are consistent with the observed inhibition profile of this series of compounds.

In conclusion, a series of mechanism-based inhibitors was used to probe the S' subsites of PR 3 and HNE. The inhibitors were found to be highly selective inhibitors of HNE and were devoid of any inhibitory activity toward PR 3. Docking studies suggest that this series of compounds binds productively to HNE but not PR 3.

Experimental

General

The ^{1}H spectra were recorded on a Varian XL-300 or XL-400 NMR spectrometer. A Hewlett-Packard diode array UV/VIS spectrophotometer was used in the *in vitro* evaluation of the inhibitors. Human neutrophil elastase, proteinase 3 and Boc-Ala-Ala-Nva thiobenzyl ester were purchased from Elastin Products Company, Owensville, MO. Methoxysuccinyl Ala-Ala-Pro-Val p-nitroanilide and 5, 5'-dithio-bis (2-nitrobenzoic acid) were purchased from Sigma Chemicals, St. Louis, MO. Melting points were determined on a Mel-Temp apparatus and are uncorrected. Reagents and solvents were purchased from various chemical suppliers (Aldrich, Acros Organics, TCI America, and Bachem). Silica gel (230–450 mesh) used for flash chromatography was purchased from Sorbent Technologies (Atlanta, GA). Thin layer chromatography was performed using Analtech silica gel plates. The TLC plates were visualized using iodine and/or UV light. Compounds **8**–**16** were generated as diastereomeric mixtures and were used as such in conducting the biochemical studies. ^{1}H NMR analysis of compound **9** showed the presence of two diastereomers (56.3% and 43.7%).

Representative Syntheses

Compound 1—Thionyl chloride (27.87 g; 234 mmol) was added dropwise to dry methanol (85 mL) cooled in an ice-salt bath. (L) Norvaline hydrochloride (25.00g; 213 mmol) was added in small portions. The ice-salt bath was then removed and the reaction mixture was heated to 40 °C for 2 h using a water bath. The reaction mixture was stirred for 2 h and the solvent was removed on the rotary evaporator, leaving a solid residue which was treated with ethyl ether (100 mL) and collected by suction filtration. The white solid (34.17 g; 96% yield) was dried in a dessiccator and used in the next step without further purification. ^{1}H NMR ($CDCI_3$): δ 0.98 (t, 3H), 1.55 (m, 2H), 2.10 (m, 2H), 3.80 (s, 3H), 4.20 (t, 1H), 8.68 (d, 3H).

Compound 2—A solution of N-chlorosulfonyl isocyanate (28.73 g; 203 mmol) in dry methylene chloride (140 mL) was cooled in an ice-water bath and a solution of t-butyl alcohol (15.05 g; 203 mmol) in dry methylene chloride (60 mL) was added dropwise with stirring. The mixture was stirred for another 15 minutes at 0 °C and the resulting mixture was added dropwise to a solution of ***1*** (34.17 g; 203 mmol) and triethylamine (1.08 g; 406 mmol)) in dry methylene chloride (200 mL) kept in an ice-water bath. The ice-water bath was removed and the mixture was stirred at room temperature overnight. The reaction mixture was then washed with 5% aqueous HCl (2 × 100 mL) and brine (100 mL). The organic layer was dried over anhydrous sodium sulfate, the drying agent was filtered off, and the solvent was removed *in vacuo* to give ***2*** (82.23 g; 100% yield) as a white solid. ^{1}H NMR ($CDCI_3$): δ 0.95 (t, 3H), 1.40 (m, 2H), 1.50 (s, 9H), 1.74 (m, 2H), 3.77 (s, 3H), 4.10 (m, 1H), 6.10 (d, 1H), 8.09 (s, 1H).

Compound 3—Compound ***2*** (62.99 g; 203 mmol) was dissolved in trifluoroacetic acid (200 mL) and the reaction mixture was stirred at room temperature overnight. Excess trifluoroacetic acid was removed using a rotary evaporator and the residue was taken up in ethyl acetate (500 mL) and washed with saturated sodium bicarbonate (5 × 150 mL) and brine (150 mL). The organic layer was dried over anhydrous sodium sulfate, the drying agent was filtered off, and the solvent was removed *in vacuo*, leaving ***3*** (33.28 g; 78% yield), as a white solid. ^{1}H NMR ($CDCI_3$): δ 0.95 (t, 3H), 1.42 (m, 2H), 1.70 (m, 2H), 3.79 (s, 3H), 4.10 (m, 1H), 5.10 (s,2H), 5.78 (d, 1H).

Compound 4—A solution of compound ***3*** (33.28 g; 158 mmol) in dry THF (300 mL) was kept in an ice-water bath and treated portion-wise with 60% w/w sodium hydride (9.48 g; 237 mmol) under nitrogen. The reaction mixture was stirred at room temperature overnight. The solvent was removed and the residue was dissolved in cold water (150 mL). The pH was

adjusted to 7 with 6 M HCl, the starting material was extracted once with ethyl acetate (150 mL), and the aqueous layer was acidified with 6 M HCl to pH 1. The product was extracted with ethyl acetate (3 × 150 mL) and the combined organic extracts were dried over anhydrous sodium sulfate. The drying agent was filtered off and the solvent was removed on a rotary evaporator, leaving product ***4*** (28.36 g; 100%), as a yellow oil. ^{1}H NMR (DMSO-d_6): δ 0.95 (t, 3H), 1.38 (m, 2H), 1.82 (m, 2H), 4.18 (q, 1H), 8.23 (m, 1H).

Compound 5—A solution of 4-chlorobenzenethiol (8.7 g; 60 mmol) in anhydrous DMF (20 mL) was treated with triethylamine (13.7g; 135 mmol) and then stirred for 15 minutes. The reaction mixture was cooled in an ice bath and ethyl 5-bromovalerate (12.55 g; 60 mmol) was added. The reaction mixture was stirred overnight and allowed to warm to room temperature. Ethyl acetate (200 mL) was added and the resulting solution was washed with 5% aqueous HCl (50 mL), 5% aqueous sodium bicarbonate (50 mL) and brine (50 mL). The organic layer was dried over anhydrous sodium sulfate, filtered, and the solvent was removed on a rotary evaporator, leaving a crude product which was purified by flash chromatography (silica gel/ethyl acetate/hexane) to give compound ***5*** (11.57 g; 71% yield) as a white solid. ^{1}H NMR ($CDCI_3$): δ 1.95 (t, 2H), 2.45 (t, 2H), 2.95 (t, 2H), 3.65 (s, 3H), 7.25 (s, 4H).

Compound 6—N-chlorosuccinimide (1.05 g; 7.85 mmol) was added in small portions over 15 minutes to a solution of compound ***5*** (2.14 g; 7.85 mmol) in benzene (10 mL) and carbon tetrachloride (10 mL) and the reaction mixture was stirred at room temperature overnight. The mixture was filtered and the filtrate was concentrated using a rotary evaporator to give compound ***6*** (1.93 g; 80% yield) as a yellow oil. The product was used in the next reaction without further purification. ^{1}H NMR ($CDCI_3$): δ 2.28 (m, 1H), 2.40 (m, 1H), 2.60 (t, 2H), 3.64 (s, 3H), 5.25 (t, 1H),7.20 (m,4H).

Compound 7—To a solution of compound ***4*** (19.6 g; 110 mmol) and triethylamine (11.13 g; 110 mmol) in anhydrous DMF (150 mL) was added compound ***6*** (30.60 g; 110 mmol) and the reaction mixture was stirred at room temperature overnight. The solvent was removed using a vacuum pump at 50 ° C. The residue was dissolved in ethyl acetate (800 mL) and washed with brine (100 mL). The organic layer was dried over anhydrous sodium sulfate, filtered, and the solvent was removed on a rotary evaporator, leaving a crude product which was purified by flash chromatography (silica gel/ethyl acetate/hexane) to give compound 7 (1.35 g; 47%) as a yellow oil. ^{1}H NMR ($CDCI_3$): δ 0.95 (m, 3H), 1.40–1.90 (m, 4H), 2.58 (m, 4H), 3.83 (m, 5H), 4.05 (m, 1H), 5.50 (m, 1H), 5.75 (s, 1H), 6.98–7.11 (m,4H).

Compound 8—A solution of compound 7 (22.98 g; 52.83 mmol) in dry acetonitrile (100 mL) was treated with 60% w/w sodium hydride (2.11 g; 52.83 mmol) at 0 ° C with stirring. After the solution was stirred for 15 minutes, methyl iodide (18.29 g; 128.85 mmol) was added and the reaction mixture was stirred for 4 h at room temperature. The solvent was removed and the residue was taken up in methylene chloride (500 mL). The organic layer was washed with water (100 mL) and then dried over anhydrous sodium sulfate. Removal of the solvent left a crude product which was purified by flash chromatography (silica gel/ethyl acetate/hexane) to give compound ***8*** (7.87 g; 33%) as a yellow oil. ^{1}H NMR ($CDCI_3$): δ 0.95 (m, 3H), 1.20–2.00 (m, 4H), 2.55 (m, 4H), 2.80 s, 3H), 3.62 (s, 3H), 3.65 (s, 3H), 5.57 (m, 1H), 7.20 (m, 4H).

Compound 9—(oil, 38%) ($CDCI_3$): δ 0.88–0.96 (m, 3H), 1.30–1.80 (m, 4H), 2.40–2.60 (m, 4H), 2.80 (s, 3H), 3.62–3.72 (m, 1H), 3.65 (s, 3H), 5.38–5.53 (m, 1H), 7.00 (t, 2H), 7.52–7.62 (m, 2H).

Compound 10—(oil, 71%) (CDCI3): δ 0.88–0.96 (m, 3H), 1.30–1.99 (m, 4H), 2.41–2.58 (m, 4H), 2.80 (s, 3H), 3.62–3.72 (m, 1H), 3.66 (s, 3H), 3.78 (s, 3H), 5.28–5.42 (m, 1H), 6.85 (d, 2H), 7.45–7.52 (m, 2H).

Compound 11—(oil, 59%) ($CDCI_3$): δ 0.88–0.96 (m, 3H), 1.20–1.98 (m, 4H), 2.42–2.55 (m, 4H), 2.80 (s, 3H), 3.62–3.70 (m, 1H), 3.64 (s, 3H), 5.22–5.35 (m, 1H), 6.60 (d, 2H), 7.38 (d, 2H).

Compound 12—(oil, 97%) ($CDCI_3$): δ 0.88–0.96 (m, 3H), 1.30–1.99 (m, 4H), 1.51 (s, 9H), 2.38–2.54 (m, 4H), 2.80 (s, 3H), 3.60–3.70 (m, 1H), 3.64 (s, 3H), 5.31–5.41 (m, 1H), 6.62 (s, 1H), 7.40 (m, 4H).

Compound 13—(oil, 74%) ($CDCI_3$): δ 0.88–0.96 (m, 3H), 1.00–2.00 (m, 4H), 2.40–2.55 (m, 4H), 2.60–2.68 (t, 2H), 2.69–2.78 (t, 2H), 2.80 (s, 3H), 3.58–3.65 (m, 1H), 3.64 (s, 3H), 5.40 (t, 1H), 7.40–7.50 (m, 4H), 8.05 (s, 1H).

Compound 14—(oil, 42%) ($CDCI_3$): δ 0.88–0.96 (m, 3H), 1.00–2.00 (m, 4H), 2.43–2.52 (m, 4H), 2.79 (s, 3H), 3.58–3.65 (m, 1H), 3.63 (s, 3H), 5.39 (t, 1H), 7.18–7.50 (m, 8H).

Compound 15—(oil, 69%) ($CDCI_3$): δ 0.88–0.96 (m, 3H), 1.00–2.00 (m, 4H), 2.43–2.56 (m, 4H), 2.79 (s, 3H), 2.81 (t, 2H), 3.48 (t, 2H), 3.60–3.70 (m, 1H), 3.63 (s, 3H), 4.80 (s, 1H), 5.36–5.40 (m, 1H), 6.40–6.44 (d, 1H), 7.18–7.45 (m, 9H).

Compound 16—(oil, 78%) ($CDCI_3$): δ 0.88–0.98 (m, 6H), 1.32–1.85 (m, 3H), 2.45–2.58 (m, 4H), 2.80 (d, 3H), 3.59–3.68 (m, 1H), 3.67 (s, 3H), 5.42–5.58 (m, 1H), 7.25 (dd, 2H), 7.45 (dd, 2H).

Enzyme assays and inhibition studies

Human neutrophil elastase—HNE was assayed by mixing 10 μL of a 70 μM enzyme solution in 0.05 M sodium acetate/0.5 M NaCl buffer, pH 5.5, 10 μL dimethyl sulfoxide and 980 μL of 0.1 M HEPES buffer containing 0.5 M NaCl, pH 7.25, in a thermostated cuvette. A 100 μL aliquot was transferred to a thermostated cuvette containing 880 μL 0.1 M HEPES/0.5 M NaCl buffer, pH 7.25, and 20 μL of a 70 μM solution of MeOSuc-Ala-Ala-Pro-Val p-nitroanilide, and the change in absorbance was monitored at 410 nm for 60 seconds. In a typical inhibition run, 10 μL of inhibitor (3.5 mM) in dimethyl sulfoxide was mixed with 10 μL of 70 μM enzyme solution and 980 μL 0.1 M HEPES/0.5 M NaCl buffer, pH 7.25, and placed in a constant temperature bath. Aliquots (100 μL) were withdrawn at different time intervals and transferred to a cuvette containing 20 μL of MeOSuc-Ala-Ala-Pro-Val p-nitroanilide (7 mM) and 880 μL 0.1 M HEPES/0.5 M NaCl buffer. The absorbance was monitored at 410 nm for 60 seconds.

Human neutrophil proteinase 3—Twenty microliters of 32.0 mM 5, 5'-dithio-bis(2-nitrobenzoic acid) in dimethyl sulfoxide and 10 μL of a 3.45 μM solution of human proteinase 3 in 0.1 M phosphate buffer, pH 6.50 (final enzyme concentration: 34.5 nM) were added to a cuvette containing a solution of 940 μL 0.1 M HEPES buffer, pH 7.25, containing 0.5 M NaCl, 10 μL 862.5 μM inhibitor in dimethyl sulfoxide (final inhibitor concentration: 8.62 μM) and 20 μL 12.98 mM Boc-Ala-Ala-NVa-SBzl and the change in absorbance was monitored at 410 nM for 2 minutes. A control (hydrolysis run) was also run under the same conditions by adding 5, 5'-dithio-bis(2-nitrobenzoic acid) in dimethyl sulfoxide and 10 μL of a 3.45 μM solution of human proteinase 3 in 0.1 M phosphate buffer, pH 6.50 (final enzyme concentration: 34.5 nM) to a cuvette containing a solution of 940 μL 0.1 M HEPES buffer, pH 7.25, containing 0.5 M NaCl, 10 μL dimethyl sulfoxide and 20 μL 12.98 mM Boc-Ala-Ala-NVa-SBzl and the

change in absorbance was monitored at 410 nM for 2 minutes. PR 3 activity remaining was determined using % remaining activity = $(v/v_o) \times 100$ and is the average of duplicate or triplicate determinations.

Computational method—Molecular docking simulations were performed via the Surflex program (30). The structure of compound ***8*** was constructed in SYBYL (31) and was structurally optimized to default convergence thresholds using the Tripos Force Field (32) and Gasteiger-Marsili partial atomic charges (33). Receptor models were prepared for HNE and PR3 using the 1HNE (34) and 1FUJ (25) crystal structures, respectively. These structures were protonated in SYBYL, stripped of all water molecules and bound ligands, and electrostatically represented with Gasteiger-Marsili charges.

Acknowledgments

This work was supported in part by a grant from the National Institutes of Health (HL 57788).

References

1. MacNee W. Proc. Am. Thorac. Soc 2004;2:258–266. [PubMed: 16267346]
2. Vandivier RW, Voelkel NF. J. Chron. Obstr. Pulmon. Dis 2005;2:177–184.
3. Senior, RM.; Shapiro, SD. Fishman's Pulmonary Diseases and Disorders. 3rd ed. McGraw-Hill, NY: 1998. COPD: Epidemiology, Pathophysiology, and Pathogenesis; p. 659-682.
4. (a) Molfino NA. Respiration 2005;72:105–112. [PubMed: 15753645] (b) Barnes PJ, Stockley RA. Eur. J. Respir. D 2005;25:1084–1106.
5. Medina-Tato DA, Watson ML, Ward SG. Drug Discov. Today 2006;11:866–879. [PubMed: 16997136]
6. Vandivier RW, Voelkel NF. J COPD 2005;2:177–184.
7. MacNee W. Proc. Am. Thor. Soc 2005;2:50–60.
8. Luppi F, Hiemstra PS. Am. J. Respir. Crit. Care Med 2007;175:527–531. [PubMed: 17407834]
9. (a) Aoshiba K, Yokohori N, Nagai A. Am. J. Respir. Cell Mol. Biol 2003;28:555–562. [PubMed: 12707011] (b) Tuder RM, Petrache I, Elias JA, Voelkel NF, Henson PM. Am. J. Respir. Cell Mol. Biol 2003;28:551–554. [PubMed: 12707010]
10. Demedts IK, Demoor T, Bracke KR, Joos GF, Brusselle GG. Respir. Res 2006;7:53–62. [PubMed: 16571143]
11. Shapiro SD, Ingenito EP. Am. J. Respir. Cell Mol. Biol 2005;32:367–372. [PubMed: 15837726]
12. Stockley RA. Am. J. Respir. Crit. Care Med 1999;260:S49–S52. [PubMed: 10556170]
13. Rennard SI. Am. J Respir. Crit. Care Med 2005;160:S12–S16. [PubMed: 10556162]
14. Pham CTN. Nat. Rev. Immunol 2006;6:541–550. [PubMed: 16799473]
15. Croxton TL, Weinmann GG, Senior RM, Hoidal JR. Am. J. Respir. Crit. Care Med 2002;165:838–844. [PubMed: 11897653]
16. (a) Morrison JF, Walsh CT. Adv. Enzymol 1998;61:201–301. [PubMed: 3281418] (b) Wakselman M, Xie J, Mazaleyrat JP. J. Med. Chem 1993;36:1539–1547. [PubMed: 8496923]
17. Silverman RB. Meth. Enzymol 1995;249:241–283.
18. (a) Groutas WC, Kuang R, Venkataraman R, Epp JB, Ruan S, Prakash O. Biochemistry 1997;36:4739–4750. [PubMed: 9125494] (b) Lai Z, Gan X, Wei L, Alliston KR, Yu H, Li YH, Groutas WC. Arch. Biochem. Biophys 2004;429:91–197. (c) Wei L, Lai Z, Gan X, Alliston KR, Lai Z, Epp JB, Tu J, Perera AB, Van Stipdonk M, Groutas WC. Arch. Biochem. Biophys 2004;429:60–70. [PubMed: 15288810] (d) Kuang R, Epp JB, Ruan S, Chong L, Venkataraman R, Tu J, He S, Truong T, Groutas WC. Bioorg. Med. Chem 2000;8:1005–1016. [PubMed: 10882012] (e) Groutas WC, Kuang R, Ruan S, Epp JB, Venkataraman R, Tu J, He S, Truong TY. Bioorg. Med. Chem 1998;6:661–671. [PubMed: 9681132] (f) Kuang R, Epp JB, Ruan S, Yu H, Huang P, He S, Tu J, Schechter NM, Turbov J, Froelich CJ, Groutas WC. J. Am. Chem. Soc 1999;121:8128–8129.

19. Nomenclature used is that ofSchechter I, Berger A. Biochem. Biophys. Res. Comm 1967;27:157–162. where S1, S2, S3,…Sn and S1', S2', S3', …Sn' correspond to the enzyme subsites on either side of the scissile bond. Each subsite accommodates a corresponding amino acid residue side chain designated P1, P2, P3, …. Pn and P1', P2', P3', …. Pn' of the substrate or (inhibitor). S1 is the primary substrate specificity subsite, and P1-P1' is the scissile bond. [PubMed: 6035483]
20. (a) Churg A, Wright JL. Curr. Opin. Pulm. Med 2005;11:153–159. [PubMed: 15699789] (b) Barnes PJ. Pharmacol. Rev 2004;56:515–548. [PubMed: 15602009] (c) Shapiro SD, Goldstein NM, Houghton AM, Kobayashi DK, Kelley D, Belaaouaj A. Am. J. Pathol 2003;163:2329–2335. [PubMed: 14633606]
21. Kao RC, Wehner NG, Skubitz KM, Gray BH, Hoidal JR. J. Clin. Invest 1998;82:1963–1973. [PubMed: 3198760]
22. (a) Bode W, Meyer E, Powers JC. Biochemistry 1989;28(1):951–1963. (b) Korkmaz B, Knight G, Bieth J. J. Biol. Chem 2003;278:12609–12612. [PubMed: 12538645] (c) Hajjar E, Korkmaz B, Gautheir F, Brandsdal BO, Witko-Sarsat V, Reuter N. J. Med. Chem 2006;49:1248–1260. [PubMed: 16480262]
23. Brubaker MJ, Groutas WC, Hoidal JR, Rao NV. Biochem. Biophys. Res. Comm 1992;188:1318–1324. [PubMed: 1445363]
24. Kam CM, Kerrigan JE, Dolman KM, Goldschmeding R, Von dem Borne AE, Powers JC. FEBS Lett 1992;297:119–123. [PubMed: 1551417]
25. Fujinaga M, Chenaia MM, Halenbeck R, Koths K, James MNG. J. Mol. Biol 1996;261:267–278. [PubMed: 8757293]
26. Huang W, Yamamoto Y, Li Y, Dou D, Alliston KR, Hanzlik RP, Williams TD, Groutas WC. J. Med. Chem 2008;51:2003–2008. [PubMed: 18318470]
27. Grob CA, Schiess PW. Angew. Chem. Int. Ed 1967;6:1–15.
28. (a) Hu WP, Wang JJ, Tsai PC. J. Org. Chem 2000;65:4208–4209. [PubMed: 10866646] (b) Wang JJ, Hu WP, Chung HW, Wang LF, Hsu MH. Tetrahedron 1998;54:13149–13154.
29. Groutas WC, He S, Kuang R, Ruan S, Tu J, Chan H-K. Bioorg. Med. Chem 2001;9:1543–1548. [PubMed: 11408173]
30. Jain AN. J. Med. Chem 2003;46:499–511. [PubMed: 12570372]
31. SYBYL 8.0. St. Louis, MO: Tripos Associates; 2008.
32. Clark M, Cramer RD III, Van Opdenbosch N. J. Comput. Chem 1989;10:982–1012.
33. Gasteiger J, Marsili M. Tetrahedron Lett 1978:3181–3184.
34. Navia MA, McKeever BM, Springer JP, Lin TY, Williams HR, Fluder EM, Dorn CP, Hoogsteen K. Proc. Natl. Acad. Sci. USA 1989;86:7–11. [PubMed: 2911584]

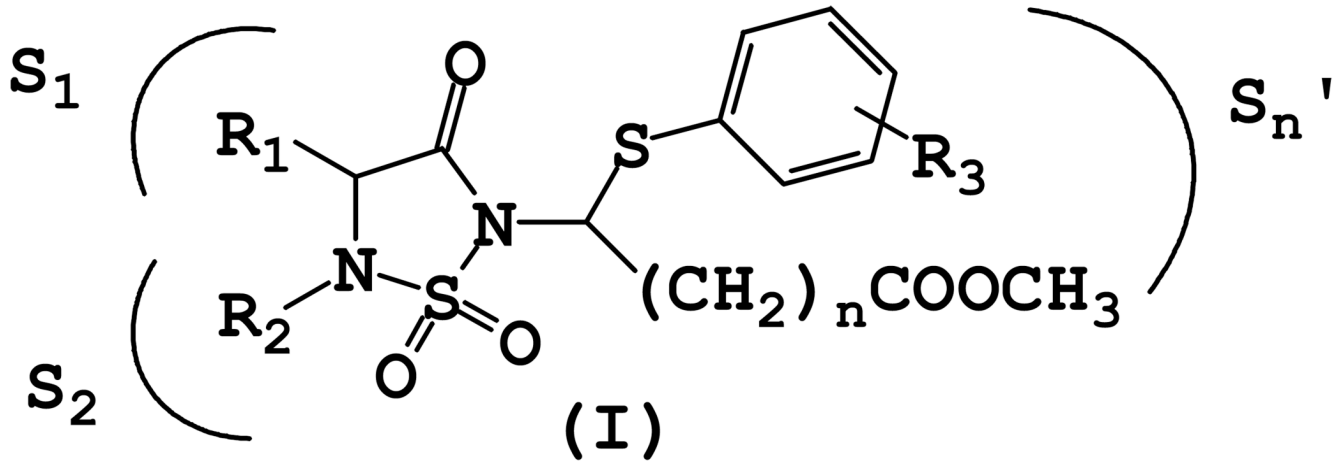

Figure 1.
General structure of inhibitor (I).

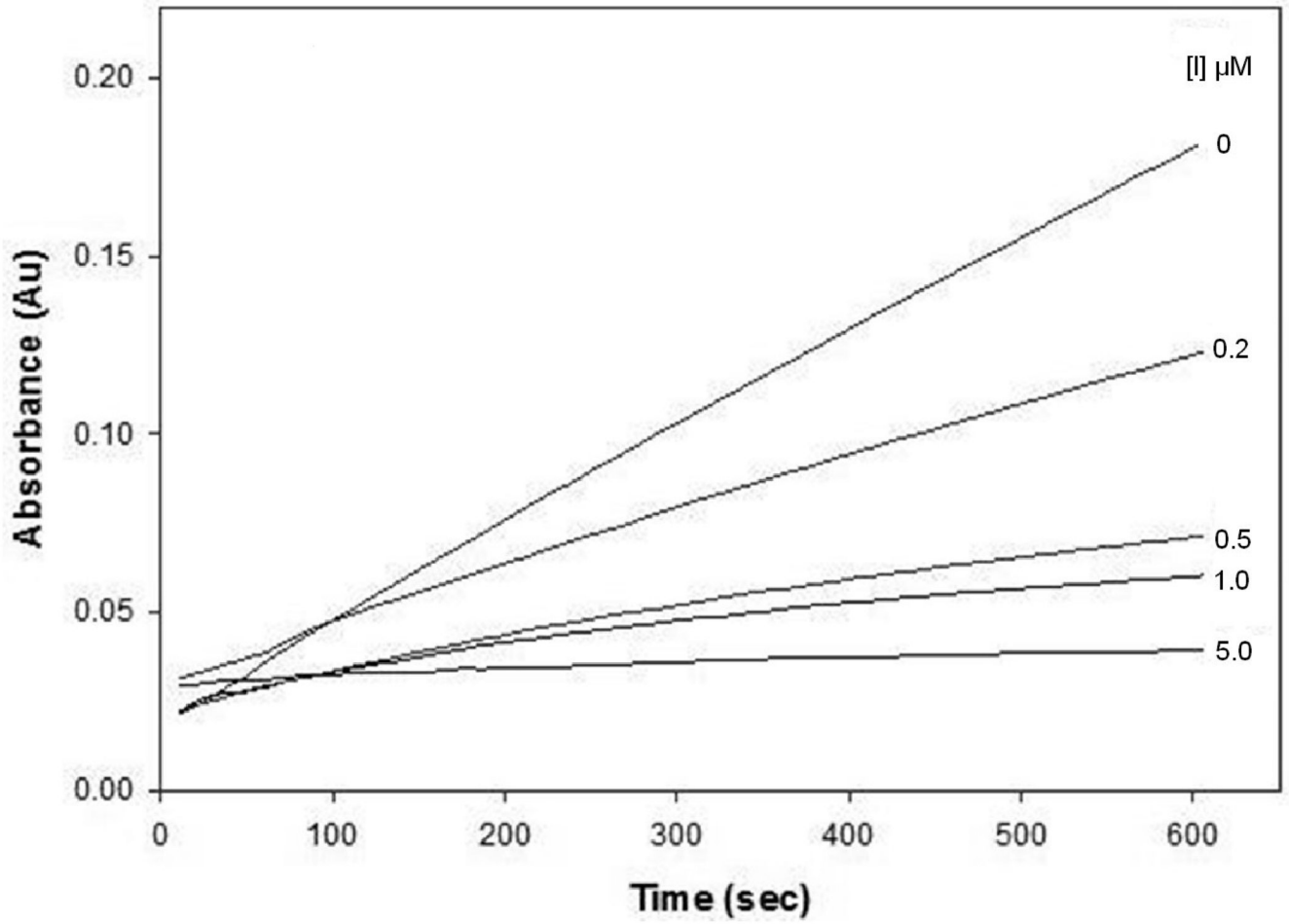

Figure 2.

Progress curves for the inhibition of human neutrophil elastase (HNE) by inhibitor ***16***. Absorbance was monitored at 410 nm for reaction solutions containing 10 nM HNE, 105 µM MeOSuc-AAPV p-nitroanilide, and the inhibitor at the indicated inhibitor to enzyme ratios in 0.1 M HEPES buffer containing 0.5 M NaCl, pH 7.25, and 2.5% DMSO. The temperature was maintained at 25°C, and reactions were initiated by the addition of enzyme.

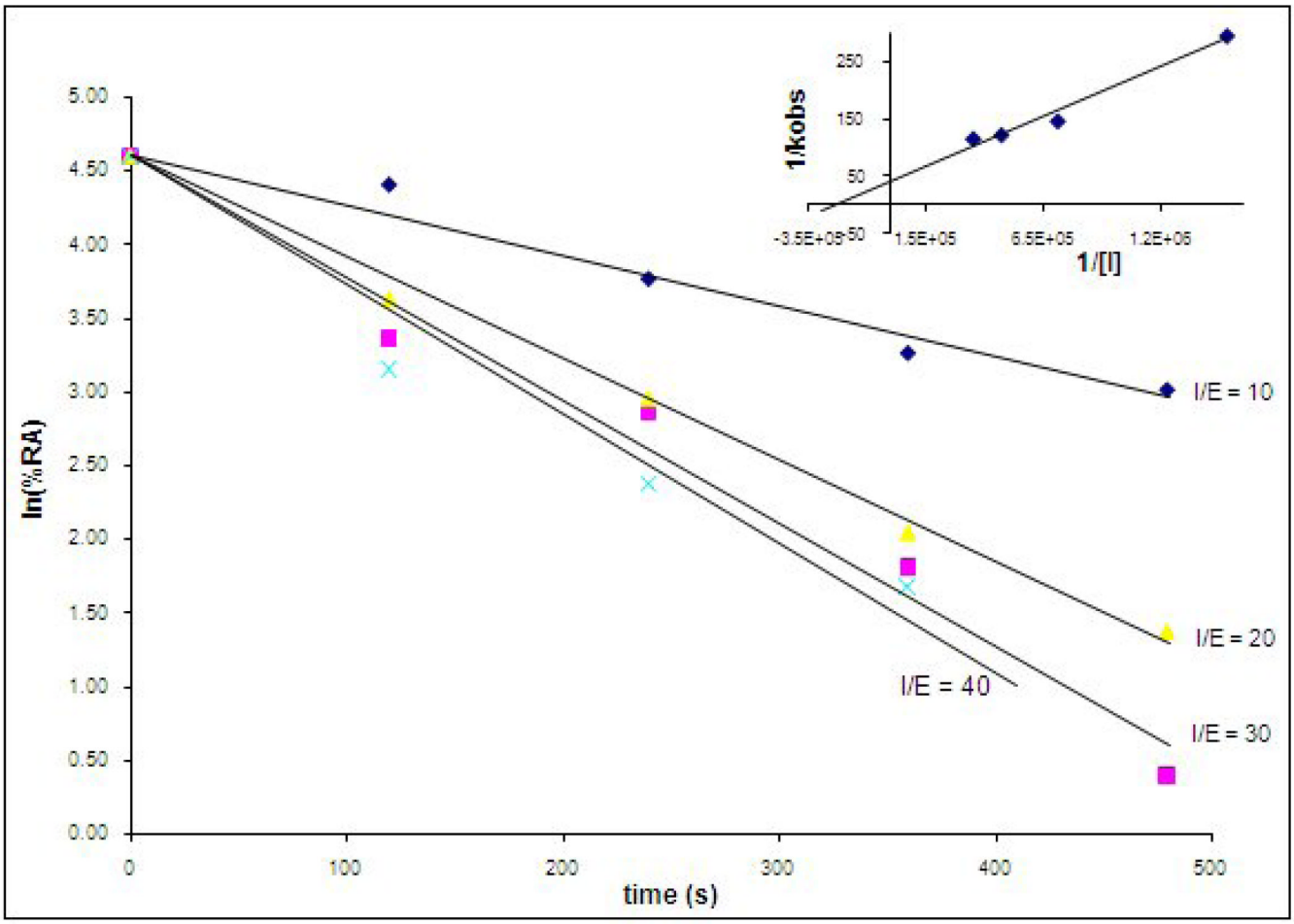

Figure 3.

Time-dependent inactivation of human neutrophil elastase (HNE) by inhibitor ***9***. HNE was incubated with inhibitor ***9*** and aliquots were withdrawn at different time intervals and assayed for enzymatic activity using MeOSuc-AAPV p-nitroanilide and monitoring the absorbance at 410 nm. ***Inset:*** Re-plot of data demonstrating saturation kinetics.

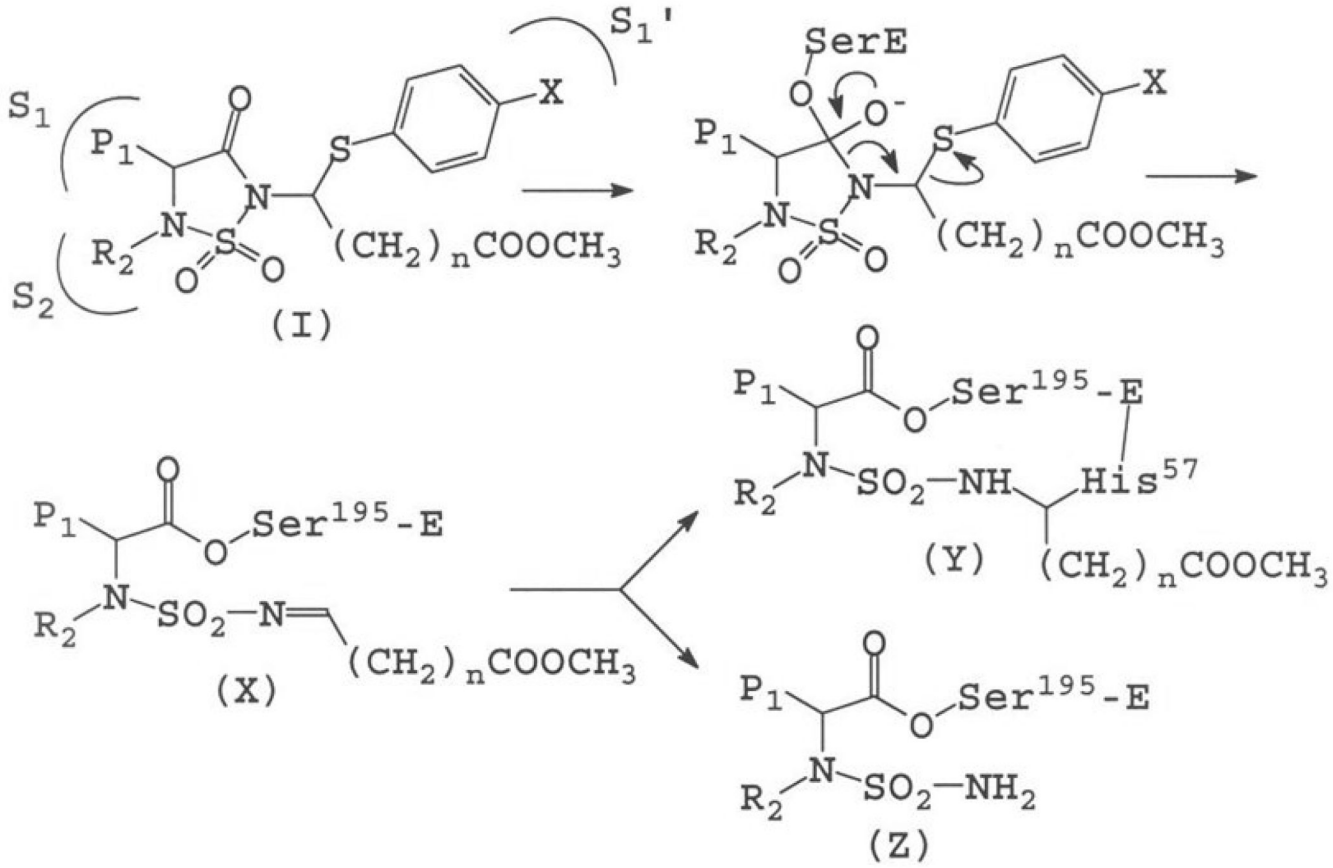

Figure 4.
Postulated mechanism of action of (I).

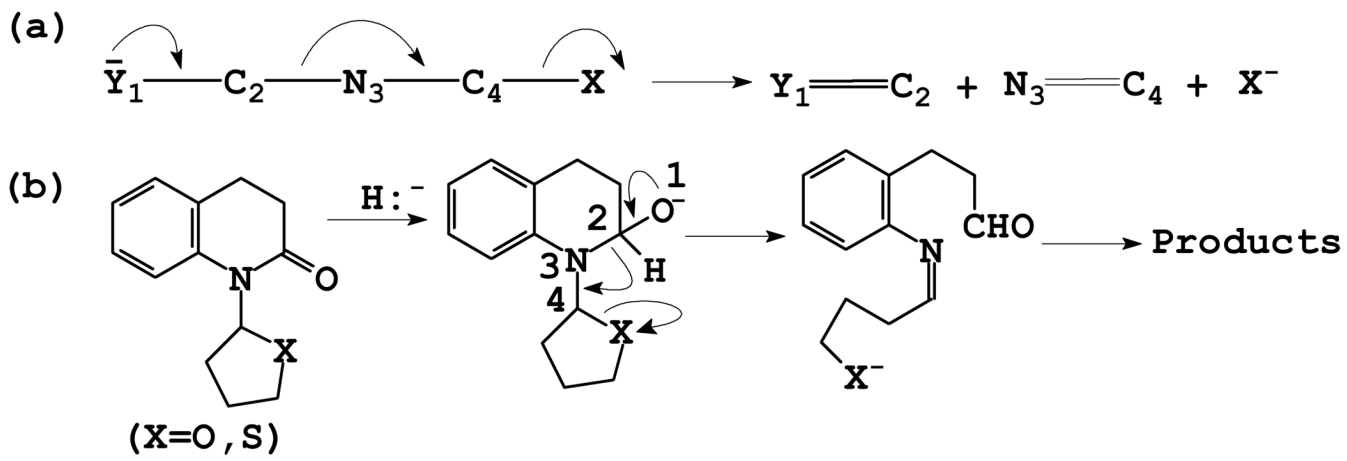

Figure 5.
(a) 3-Aza Grob fragmentation; (b) Amide bond cleavage via a 3-aza Grob fragmentaion process.

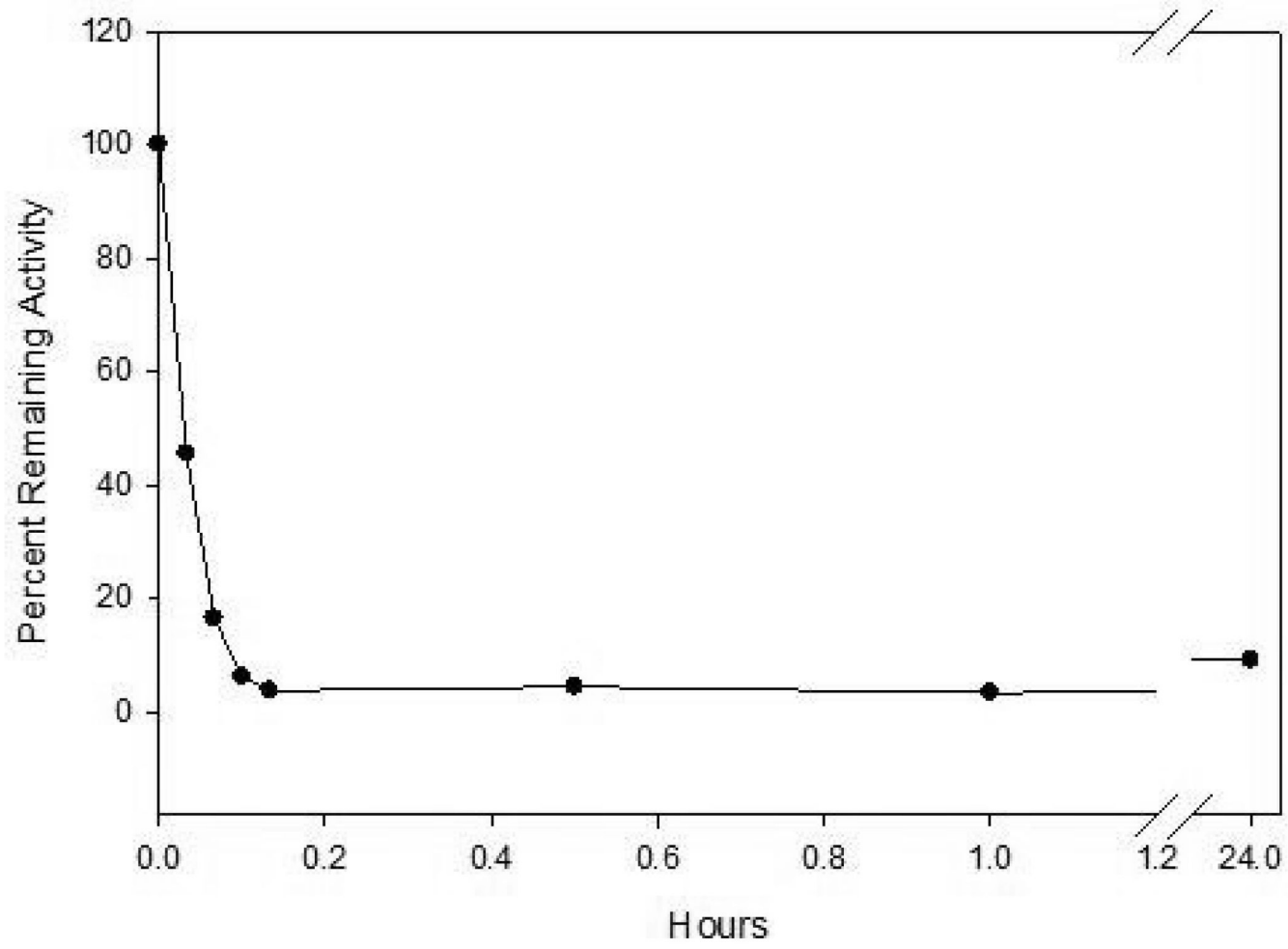

Figure 6.

Time dependent loss of enzymatic activity. Percent remaining activity versus time plot obtained by incubating inhibitor ***16*** (37 μM) with human neutrophil elastase (700 nM) in 0.1 M HEPES buffer containing 0.5 M NaCI, pH 7.25, and 1% DMSO. Aliquots were withdrawn at different time intervals and assayed for enzymatic activity using MeOSuc-AAPV p-NA by monitoring the absorbance at 410 nm.

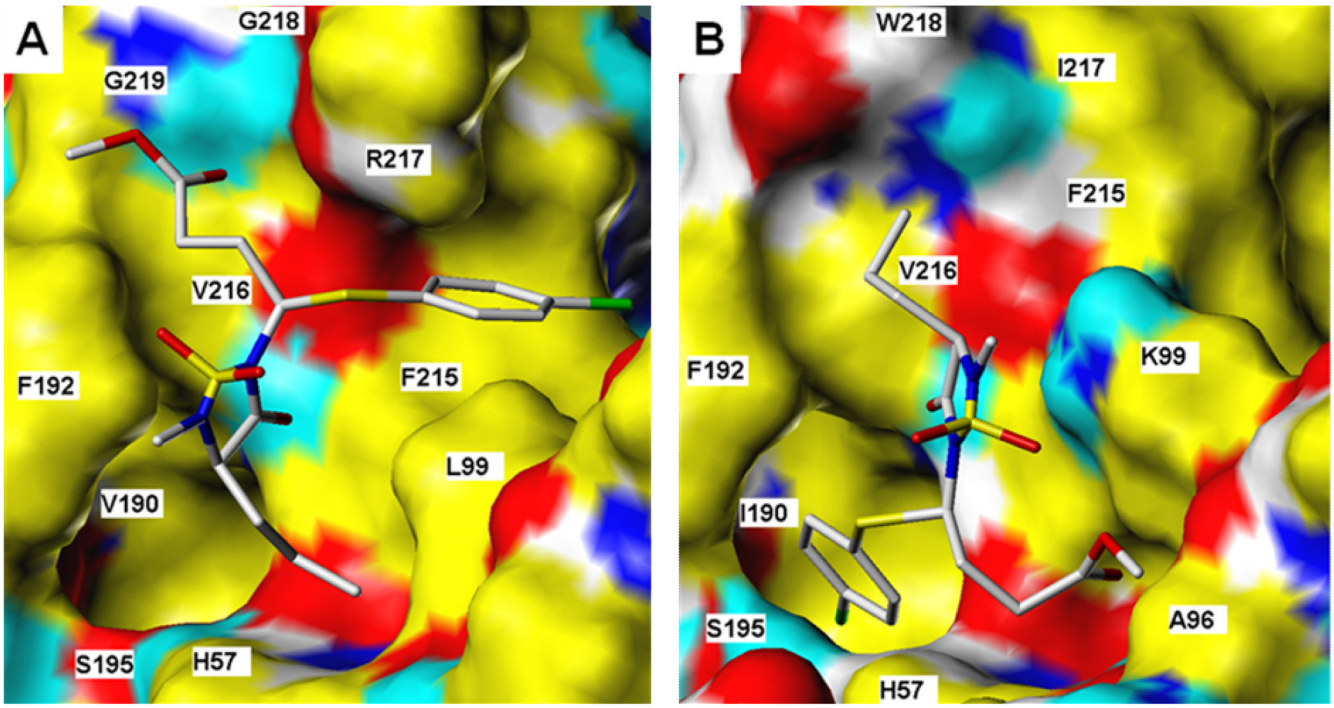

Figure 7.
Inhibitor ***8*** bound to a) HNE and b) PR3. Ligand rendered as CPK-colored sticks. Receptor surface colors correspond to: yellow = non-polar, white = polar alkyl, blue = polar N, cyan = polar H, red = O.

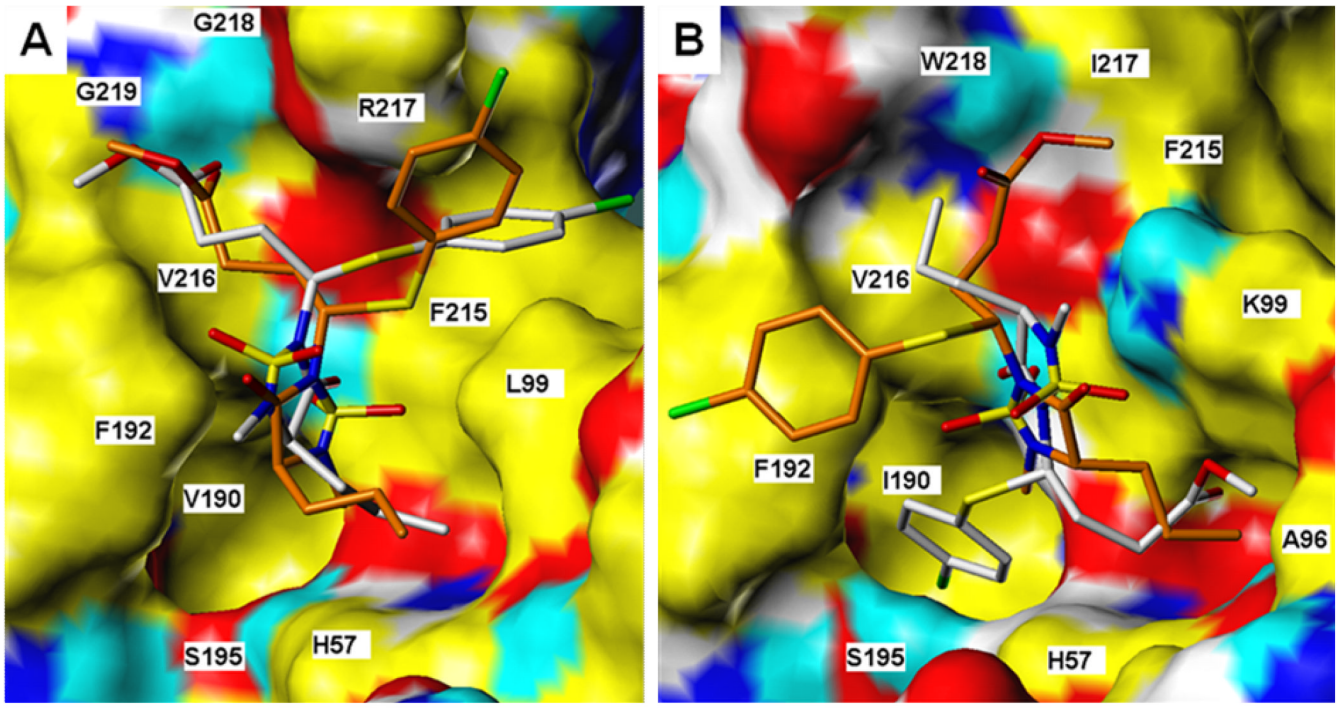

Figure 8.
RR and SS isomers of inhibitor ***8*** bound to a) HNE and b) PR 3. Ligand rendered as CPK-colored sticks (RR has grey C's; SS has green). Receptor surface: yellow = non-polar, white = polar alkyl, blue = polar N, cyan = polar H, red = O.

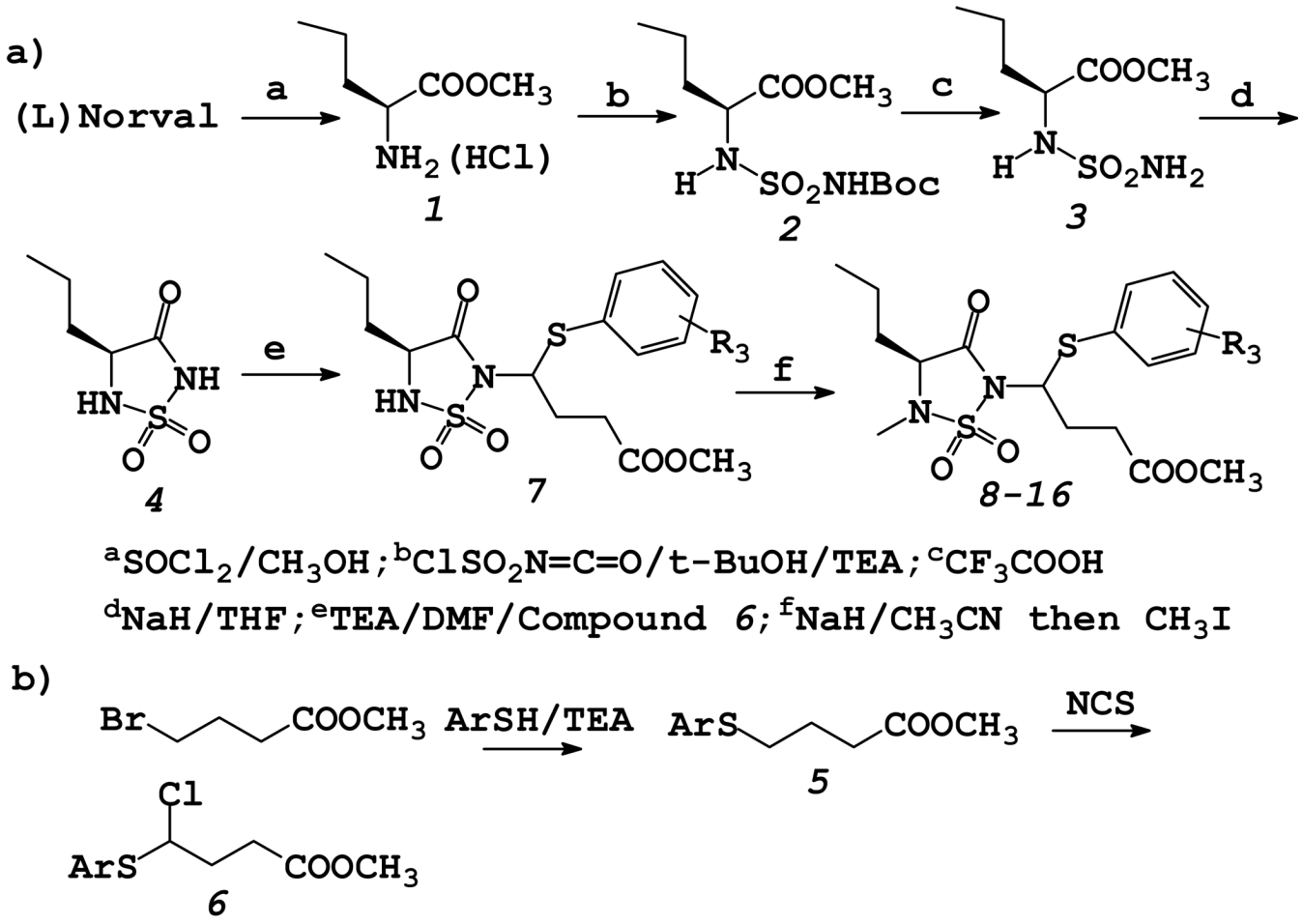

Scheme 1.
Synthesis of Inhibitors 8–16

Table 1

Inhibition of human neutrophil elastase by derivatives of compound (I)[ab]

Compound	R_3	$k_{obs}/[I]$ M^{-1} s^{-1}
8	p-Cl	20
9	p-F	320
10	p-OCH_3	70
11	p-NH_2	110
12	p-NHBoc	170
13	p-$NHCO(CH_2)_2COOH$	300
14	p-$NHCO(o\text{-}COOH)C_6H_4$	260
15	p-$NHCONH(CH_2)_2Ph$	150
16[c]	p-Cl	4580[d]

[a] R_1=n-propyl, R_2=methyl for all, unless indicated otherwise;

[b] used as diastereomeric mixtures;

[c] R_1=isobutyl, R_2=methyl;

[d] determined using the progress curve method and expressed as k_{inact}/K_I M^{-1} s^{-1} (see Experimental section).